Fish and Shellfish Immunology 92 (2019) 570–582

Contents lists available at ScienceDirect

Fish and Shellfish Immunology

journal homepage: www.elsevier.com/locate/fsi

Full length article

Identification and molecular characterization of peroxiredoxin 2 in grass carp (*Ctenopharyngodon idella*)

Denghui Zhu[a,b], Rong Huang[a], Cheng Yang[a,b], Peipei Fu[a,d], Liangming Chen[a,b], Yinjun Jiang[a,b], Libo He[a], Yongming Li[a], Lanjie Liao[a], Zuoyan Zhu[a], Yaping Wang[a,c,*]

[a] State Key Laboratory of Freshwater Ecology and Biotechnology, Institute of Hydrobiology, Chinese Academy of Sciences, Wuhan, 430072, China
[b] University of Chinese Academy of Sciences, Beijing, 100049, China
[c] Innovative Academy of Seed Design, Chinese Academy of Sciences, Beijing, 100101, China
[d] Key Laboratory of Aquaculture Disease Control, Ministry of Agriculture, And State Key Laboratory of Freshwater Ecology and Biotechnology, Institute of Hydrobiology, Chinese Academy of Sciences, Wuhan, 430072, China

ARTICLE INFO

Keywords:
Grass carp
Recombinant protein
Peroxiredoxin 2 (Prx2)
Subcellular localization
Gene expression
Antioxidant activity
Immune response

ABSTRACT

Peroxiredoxin (Prx), also named thioredoxin peroxidase (TPx), is a selenium independent antioxidant enzyme that can protect organisms from oxidative damage caused by reactive oxygen species (ROS) and is important for immune responses. In this study, the molecular cloning and characterization of a Prx2 homologue (*CiPrx2*) were described from grass carp (*Ctenopharyngodon idella*). The full-length cDNA of *CiPrx2* was 1163 bp containing 5′-untranslated region (UTR) of 52 bp, a 3′-UTR of 517 bp with the putative polyadenylation consensus signal (AATAAA), an open reading frame (ORF) of 594 bp encoding polypeptides of 197 amino acids with a predicted molecular mass of 21.84 kDa and theoretical isoelectric point of 5.93. The analysis results of multiple sequence alignment and phylogenetic tree confirmed that *CiPrx2* belong to the typical 2-Cys Prx subfamily. The *CiPrx2* mRNA was ubiquitously expressed in all tested tissues. The temporal expression of *CiPrx2* were differentially induced infected with grass carp reovirus (GCRV), polyinosinic:polycytidylic acid (poly I:C) and lipopolysaccharide (LPS) in liver and spleen. Subcellular localization of CiPrx2-GFP fusion proteins were only distributed in the cytoplasm. The purified recombinant CiPrx2 possessed an apparent antioxidant activity and could protect DNA against oxidative damage. Finally, CiPrx2 proteins could obviously inhibit H_2O_2 and heavy metal toxicity. However, further researches are needed to better understand the regulation of CiPrx2 under oxidative stresses.

1. Introduction

Reactive oxygen species (ROS), such as superoxideanion (O^{2-}), hydrogen peroxide (H_2O_2) and hydroxyl radical (OH.) [1], are produced in eukaryotic cells mainly by mitochondria as a byproducts of aerobic respiration and associated redox reactions. Low levels of ROS are necessary for the normal cellular functions, involved in regulation of gene expression [2], intracellular signal transduction [3], host defense against pathogenic infections [4] and so on. Though the production of ROS is an important host defense mechanism for killing invading pathogens, the mass accumulation of ROS might cause serious oxidative damage to biological macromolecules, associated with various diseases, such as nucleic acid damage, protein oxidation, lipid peroxidation and modification of lipoproteins [4–8]. To minimize the oxidative stress, organisms have evolved protective enzymatic systems [9]. These enzymatic antioxidants include superoxide dismutase (SOD), catalase (CAT), glutathione peroxidase (GSH-Px) and peroxiredoxins (Prxs) [10].

Peroxiredoxins (Prxs), also named thioredoxin peroxidase (TPx), is a selenium independent peroxidase protein that catalyze/reduce the cytokine induced peroxides and its activity is regulated by thioredoxin [11]. Prxs exist ubiquitously in most species from prokaryotes to eukaryotes [12]. Based on the number of conserved cysteine residues, the Prx superfamily had been divided into typical 2-Cys Prxs (Prx1-Prx4) (Prx1 and Prx2 were also named as natural killer enhancing factor (NKEF)-A and NKEF-B, respectively), 1-Cys Prx (Prx6) and atypical 2-Cys Prxs (Prx5) [13]. Prx proteins played important roles in some cellular functions, such as involved in protein and lipid protection against oxidative injury [14], intracellular signaling pathways regulating apoptosis [15], cell proliferation, differentiation [16,17], and anti-viral activity in vitro [18].

Prx2, a member of peroxiredoxin family, have been cloned from

* Corresponding author. Institute of Hydrobiology, Chinese Academy of Sciences, Wuhan, 430072, China.
E-mail address: wangyp.ihb@gmail.com (Y. Wang).

https://doi.org/10.1016/j.fsi.2019.06.022
Received 18 March 2019; Received in revised form 10 June 2019; Accepted 11 June 2019
Available online 14 June 2019

many fish species, such as common carp *Cyprinus carpio* [19,20], pufferfish *Tetraodon nigroviridis* [21], southern bluefin tuna *Thunnus maccoyii* [22], Miiuy croaker *Miichthys miiuy* [23,24] and black carp *Mylopharyngodon piceus* [25]. The research results of the literature abovementioned revealed the fact that Prx2 were involved in the immune response against pathogen infection.

In this report, we described the molecular cloning and characterization of a Prx2 homologue (*CiPrx2*) from grass carp (*Ctenopharyngodon idella*), one of the most important cultured fish species in China [26]. The expression profiles of *CiPrx2* mRNA were studied after infection with pathogen-associated molecular patterns (PAMPs) and GCRV challenge. Functional role of *CiPrx2* was investigated (in *vitro*) using recombinant CiPrx2 as an antioxidant enzyme.

2. Materials and methods

2.1. Ethics statement

All animal experiments were complied with the ARRIVE guidelines and were carried out in accordance with the National Institutes of Health guide for the care and use of Laboratory animals (NIH Publications No. 8023, revised 1978). All surgeries were performed under eugenol anesthesia (final concentration: 100 mg/l) and all efforts were made to minimize suffering. All protocols were approved by the committee of the Institute of Hydrobiology, Chinese Academy of Sciences (CAS). The reference number obtained was Y11201-1-301 (Approval date: 30 May 2016).

2.2. Fish and challenge experiment

Grass carps (3-month-old; weight, 10 ± 2 g; length, 7 ± 3 cm) were collected at the GuanQiao Experimental Station, Institute of Hydrobiology, Chinese Academic of Sciences, and acclimatized in aerated freshwater at 28 °C for one week. The fish were fed with a commercial feed (Tong Wei, Chengdu, China) to adapt to the environment until 24 h before the experiments under the same conditions. For the tissue distribution experiment, ten tissue types, including liver, muscle, spleen, gill, intestine, skin, head kidney, middle kidney, heart and brain, were collected from 5 random untreated grass carp.

The GCRV challenge experiment was performed as described previously [27] with some modifications. Briefly, 5 healthy grass carps were intraperitoneally injected with 200 μl PBS (pH 7.4) as control group while fish of challenge group were injected with an equal volume of GCRV (GD108 strain). The titer of virus detected by RT-qPCR (the special primers were listed in Table 1) was 3.12×10^3 copy/μl. These injected fish were kept under the same conditions as above mentioned. Five individuals were collected at the indicated times post-infection, including 0, 1, 2, 3, 4, 5 and 6 days post injection (dpi). The spleen and liver were harvested into TRIzol reagent (Invitrogen, Carlsbad, CA, USA) and stored at −80 °C until RNA extraction.

Table 1
Primers used in this study.

Primers	Sequences (5′—3′)	Purpose
Prx2-5′Rout	TGCACCAGTCTCAGAGTCTCGTC	5′ RACE
Prx2-5′Rin	AGCGATGACCTCACAGCCG	
Prx2-3′Rout	TCTACCCGCTTGATTTCACCTTC	3′ RACE
Prx2-3′Rin	GTTCTGAAAGAGGAGGAGGGCA	
Prx2-F	ATGTCTGCTGGAAACGCTAAGAT	ORF cloning
Prx2-R	TTACTGCTTGGAGAAGAACTCCTT	
qPrx2-F	TCTACCCGCTTGATTTCACCTTC	RT-qPCR
qPrx2-R	AGCGATGACCTCACAGCCG	
qβ-actin-F	TCGGTATGGGACAGAAGGAC	
qβ-actin-R	GACCAGAGGCATACAGGGAC	
qS6-F	AGCGCAGCAGGCAATTACTATCT	GCRV RT-qPCR
qS6-R	ATCTGCTGGTAATGCGGAACG	

For PAMPs challenge experiment, 150 grass carps were randomly divided into three groups, control group, LPS and poly I:C challenge groups. The 50 individuals of control group were intraperitoneally injected with 200 μl PBS (pH 7.4) while 50 individuals of each challenge groups were also intraperitoneally injected with an equal volume of LPS (L2880, Sigma, St. Louis, MO, USA, from *Escherichia coli* 055: B5, 0.5 mg/ml) or 200 μl poly I:C (27472901, GE, 1 mg/ml) dissolved in PBS. These injected fish were kept under the same conditions as above mentioned. At 3, 6, 12, 24, and 48 h post-injection (hpi), 5 individuals from each group were anaesthetized in eugenol anesthesia (final concentration: 100 mg/L). The spleen and liver were harvested into TRIzol reagent (Invitrogen) and stored at −80 °C until RNA extraction.

2.3. Cloning of the CiPrx2 cDNA

Total RNAs were extracted using TRIzol reagent according to the manufacture's protocol (Invitrogen). RNA samples were incubated in RNase-free DNase I (Promega, Wisconsin, USA) to eliminate any contaminating genomic DNA. First-strand cDNA synthesis was carried out based on ReverTra Ace kit (Toyobo, Osaka, Japan) using oligo (dT)-adaptor as primer. The reaction was performed at 42 °C for 1 h, and terminated by heating at 95 °C for 5 min.

The specific fragments with the coverage of ORF region of were obtained by blasting the Prx2 sequence of zebrafish (Accession no. NM_001002468.2) with the *C. idella* transcriptional database [28]. Following, the ORF sequence was amplified using one pair of primers (Table 1), and then specific and adaptor primers (Table 1) were designed to clone the 5′ and 3′ UTRs using rapid-amplification of cDNA ends (RACE). This experiment was performed using the 5′ and 3′ Full RACE Kit (TaKaRa, Kusatsu, Japan). PCR products were ligated into pMD18-T vectors (Takara, Japan) and transformed to *E. coli* DH5α (TransGen Biotech, Beijing, China) for sequencing by a commercial company (Tsing Ke, Wuhan, China). Finally, the ORF sequence and the 5′- and 3′-UTR sequences were assembled to obtain the *CiPrx2* full length cDNA using DNAMAN software.

2.4. Bioinformatic analysis of CiPrx2

The full-length cDNA sequences of *CiPrx2* were blasted for homology using the Basic Local Alignment Search Tool at the National Center for Biotechnology Information (NCBI) (http://blast.ncbi.nlm.nih.gov/Blast). The nucleotide and predicted amino acid sequences of CiPrx2 were analyzed using The Sequence Manipulation Suite (SMS) (http://www.bio-soft.net/sms/). The functional domains of the deduced amino acid sequence were predicted using on line SMART (http://smart.emblheidelberg.de/) [29]. The online SignaIP 4.0 Server (http://www.cbs.dtu.dk/services/SignalP/) was used to predict the signal peptide. The molecular weight (MW) and the isoelectric point (pI) of the deduced amino acid sequences were calculated by ExPASy (http://web.expasy.org/compute_pi/). The amino acid sequence of CiPrx2 was comparatively analyzed with orthologous sequences by software Geneious 8.0. The ClustalW2 (http://www.ebi.ac.uk/Tools/msa/clustalw2/) tool was engaged in performing the multiple sequences alignment. The phylogenetic position of CiPrx2 was assessed by reconstructing a phylogenetic tree using MEGA 5.0 program based on neighbor-joining (NJ) method with 1000 bootstraps [30].

2.5. Expression analysis of CiPrx2 by RT-qPCR

The RNA extraction and cDNA synthesis were performed as described previously [31]. All the samples of RNA were extracted from TRIzol reagent. 2 μg total RNA was used for synthesizing first-strand cDNAs and oligo (dT) primers in 20 μl reaction solution.

In order to understand the expression profiles of *CiPrx2* in different tissues and transcriptional regulation of immune challenged animals,

Quantitative real-time PCR (RT-qPCR) was carried out using iQ™ SYBR Green Supermix (Bio-Rad, Hercules, CA, USA) on a CFX96™ Real Time Detection System (Bio-Rad). A pair of gene-specific primers (Table 1) were used to amplify the *CiPrx2* fragment. The β-actin (Accession No. M25013.1) was selected as internal control and amplified with its specific primers (Table 1). The RT-qPCR cycling conditions were as follows: 95 °C for 2 min, 40 cycles of 95 °C for 10 s, annealing at 62 °C for 20 s, and 72 °C for 30 s, followed by a Melt Curve was constructed. Finally, the Ct values for respective reaction were subjected to comparative Ct method ($2^{-\Delta\Delta CT}$) [32] to calculate the *CiPrx2* mRNA levels. Data are expressed as the *CiPrx2* expression-fold relative to that of β-actin mRNA (expressed as mean (M) ± standard deviation (SD)). To test the effectiveness of GCRV infection, the relative copy number of the virus in gill were examined by RT-qPCR. The expression level of day 1 was set as the baseline (1.0). The special primers were designed based on the S6 segments of GCRV-II (special primers in Table 1). Statistical analysis was conducted using one-way ANOVA by SPASS 16.0 and a probability level of $p \leq 0.05$ was considered as statistically significant.

2.6. Plasmid construction, recombinant expression and purification of CiPrx2 protein

To purify the recombinant CiPrx2, the cDNA fragment encoding the mature peptide of CiPrx2 was amplified with specific primers (Table 2), then ligated into pEASY-Blunt cloning vector (TransGen Biotech). The recombinant plasmid was transformed into *E. coli* BL 21 (transsetta DE3) competent cells (TransGen Biotech), and confirmed by sequencing. *E. coli* BL21 transformed cells were cultured in 500 ml lysogeny broth (LB) with ampicillin (100 μg/ml) at 37 °C until ~0.6 OD600 reached. Cells were induced with isopropyl-β-thiogalactopyranoside (IPTG) at a final concentration of 1 mM for 10 h at 20 °C. Then, cells were kept on ice for 30 min and pelleted by centrifugating (4000 × *g* for 20 min at 4 °C). Pelleted cells were resuspended in column buffer (20 mM Tris–HCl, pH 7.4, 200 mM NaCl) and stored overnight at −20 °C. Cell suspension was thawed and sonicated on ice in the presence of phenylmethane sulfonyl fluoride (PMSF, 1 mg/ml) protease inhibitor cocktail (Beyotime, Shanghai, China). Cells lysis was subjected to centrifugation (20,000 × *g* for 20 min at 4 °C) and the supernatant was purified with NI-NTA resign (TransGen Biotech). The recombinant proteins were analyzed by 12% SDS-PAGE and then transferred to a polyvinylidene difluoride (PVDF) membrane (Millipore, Massachusetts, USA) using a Mini *Trans*-Blot electrophoretic transfer system (Bio-Rad). Membranes were blocked with 5% non-fat milk (diluted with PBS containing 0.1% Tween-20) (PBST) for 2 h at room temperature, and then incubated with anti-His tag antibodies (diluted 1: 5000 with 5% non-fat milk in PBST) for 8 h at 4 °C. After washing with PBST, the membranes were incubated with goat anti-rabbit IgG (Beyotime) (diluted 1: 5000 with 5% non-fat milk in PBST) for 1 h at room temperature. The immunoblot signals were detected using an HRP-DAB Detection Kit (Tiangen, Beijing, China). Concentration of the purified protein was determined by using the BCA Protein Assay Kit (Novagen, Hilden, Germany). The gels were visualized by Comassie blue R-250 staining.

2.7. Mixed-function oxidase assay

Mixed-Function Oxidase (MFO) assay was used to investigate the antioxidant potential of CiPrx2 according to described previously [33] with some modifications. The MFO assay was used to determine the degree of DNA breakage caused by the ROS generated from the thiol/Fe^{3+}/O_2^- MFO system and to what extent the CiPrx2 could inhibit the DNA breakage. The assay was performed in a total reaction volume of 30 μl with 10 μM $FeCl_3$, 10 mM DTT and different concentrations of purified rCiPrx2 fusion protein. Thereafter, mixtures were incubated at 37 °C for 1 h. After incubation, 1 μg of pEGFP-N3 super coiled DNA was added to each reaction mixture and incubated further at 37 °C for 1 h. Finally, reaction mixtures were purified and analyzed using 1% agarose gel. The agarose gel was stained with ethidium bromide and visualized under UV light. Triplicated assays were performed to confirm the reliability.

2.8. H_2O_2 and heavy metal toxicity stress resistance properties assays in vitro

The functional response of CiPrx2 to H_2O_2 and heavy metals toxicity stress was evaluated by agar diffusion test method. The agar diffusion test method was described previously [34] with some modifications. *E. coli* BL21 cells transformed with pEASY-CiPrx2 vector were considered as experimental group and pEASY-Blunt empty vector were considered as control group. Both of them were cultured in 5 ml LB with ampicillin (100 μg/ml) at 37 °C until ~0.6 OD_{600} reached then induced for 3 h with IPTG. Two groups of agarose plates were coated with the 200 μl above of bacterial liquid respectively. Sterile filter papers (diameter: 6 mm) were firstly soaked with 1 mol/l concentrations of copper, zinc, chromium and ferrum, and then were put on the agarose plates cultured overnight. The sterile filter papers were also saturated by H_2O_2 with a concentration of 30%, 20%, 15%, 10%, 6%, 3% severally. Meanwhile, the sterile filter paper soaked with PBS worked as control. Finally, these soaked sterile filter papers were placed on the two groups of agarose plates, respectively. All the agarose sugar plates above were trained overnight at a constant temperature of 37 °C. Then the clearing zone diameters were measured and compared between *E. coli* BL21 with recombinant plasmid pEASY-CiPrx2 and only pEASY-Blunt empty vector which were stimulated with heavy metals and H_2O_2.

2.9. Subcellular localization

Human embryonic kidney 293T (HEK 293T) cells were cultured at High glucose Dulbecco's modified Eagle's medium (DMEM; Hyclone, Logan, UT, USA), with 10% fetal bovine serum (FBS), 100 IU/ml penicillin (Sigma) and 100 mg/ml streptomycin (Sigma) under a humidified condition with 5% CO_2 at 37 °C.

For the aim to investigate the subcellular localization, pEGFP-N3 (Clontech, Palo Alto, California, USA) was used as the original plasmid. Specific primer pairs containing *Xho*I and *Bam*HI, restriction enzyme cutting sites (Table 2) were designed to amplify the complete ORF sequence of CiPrx2. After digested by restriction enzyme, the PCR product was cloned into pEGFP-N3 vectors producing GFP-tagged expression plasmids. Finally, sequence of the resulting plasmid was verified by DNA sequencing. HEK293T cells were seeded into a sterile microscope

Table 2
Primers used in this study.

Primers	Sequences (5′—3′)	Purpose
pEGFP-Prx2-F	CGCTCGAGGTATGTCTGCTGGAAACGCTAAGAT	Subcellular localization
pEGFP-Prx2-R	CGGGATCCCTGCTTGGAGAAGAACTCCTT	
pEASY-Prx2-F	ATGTCTGCTGGAAACGCTAAGAT	Recombinant expression
pEASY-Prx2-R	TTACTGCTTGGAGAAGAACTCCTT	

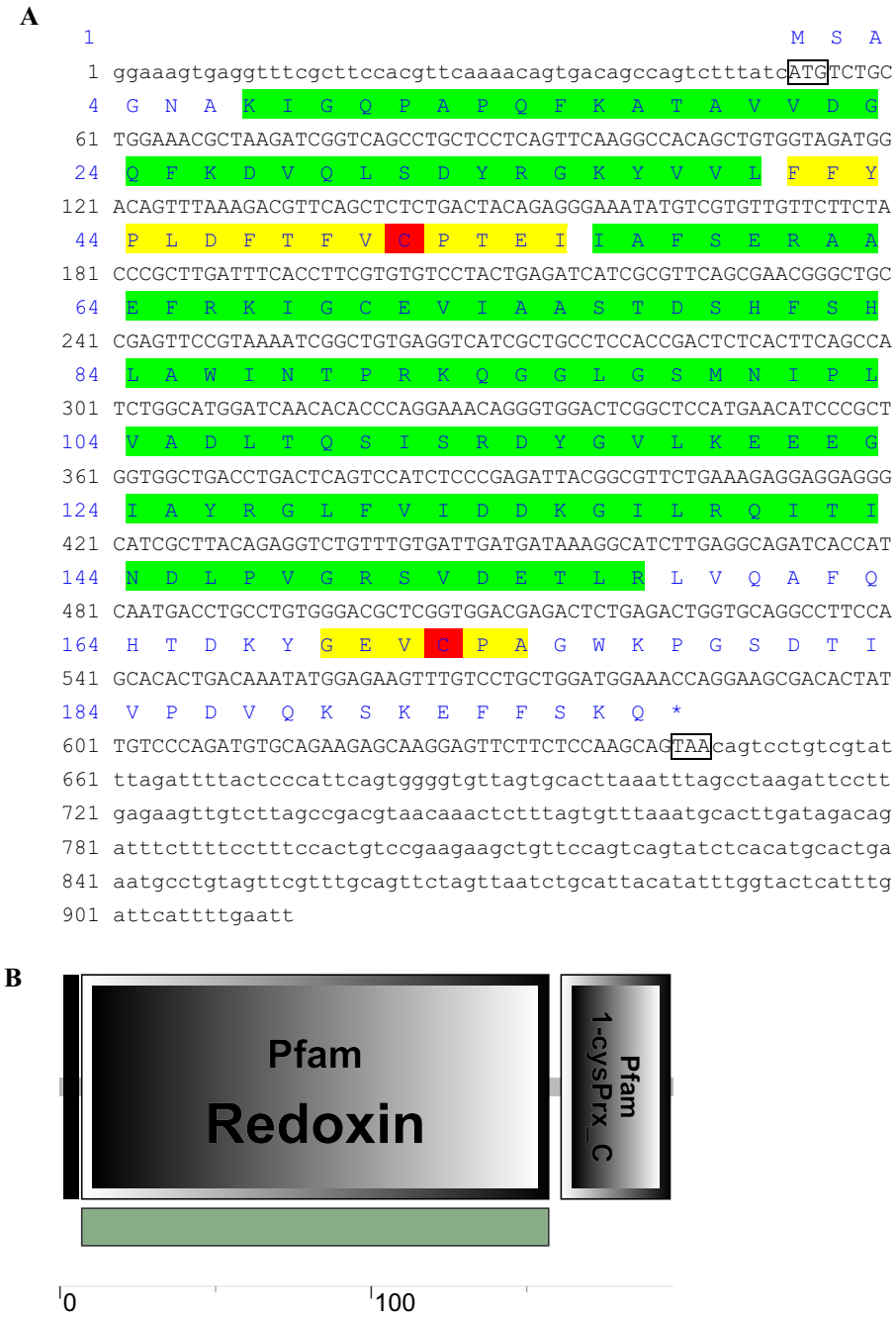

Fig. 1. (A) The nucleotide and deduced amino acid sequence of the *CiPrx2* gene. The nucleotide sequence (lower) and the deduced amino acid sequence (upper) were numbered. Start codon (ATG) and the stop codon (TAA) were boxed. The redoxin domain and Prx signature motifs (FFYPLDFTFVCPTEI and GEVCPA) were colured in bright green and yellow, respectively, and the two active cysteines were red shaded. (B) Schematic diagram of CiPrx2 functional domains. (For interpretation of the references to colour in this figure legend, the reader is referred to the Web version of this article.)

cover glass and placed in a 6-well cell culture plate prior to transfection. After cells grown at 70–90% confluence, 5 μg of pEGFP-N3-CiPrx2 vectors were transiently transfected, empty pEGFP-N3 vector was used as the control. Transfection of plasmids in HEK 293T cells was performed using Lipo 6000™ Transfection Reagent (Beyotime). After transfection for 24 h, the cells were washed three times with PBS and fixed with 4% (v/v) paraformaldehyde for 15 min at room temperature. Then, the cells were dyed with Hoechst 33342 (Beyotime) and observed under the UltraVIEW VOX confocal system (PerkinElmer, Fremont, CA, USA) and a 63× oil immersion objective lens. Subsequently, the cells were collected and lysed for the confirmation of CiPrx2-GFP fusion protein by Western blotting, with the primary antibody (Anti-GFP) diluted at 1: 5000. The immunoblot signals were detected as described in 2.6.

2.10. Statistical analysis

All the data were analyzed using the SPSS 16.0 (IBM Corporation, Armonk, NY, USA) and assessed by one-way analysis of variance (ANOVA). All the experiments were repeated at least three times. The significance level was set at $p \leq 0.05$ and the extreme significance level was set at $p \leq 0.01$.

Table 3
Amino acid sequence similarity of CiPrx2 with other species by Geneious.

Percents of similarity		1	2	3	4	5	6	7	8	9	10	11	12	13	14	15	16	17	18	19	20	21	22	23	24
Percents of similarity	1. M.musculus_Prx2		98.5	93.4	86.4	76.1	75.6	75.6	76.6	76.1	77.2	76.1	77.2	76.6	76.6	78.7	67.3	74.4	75.9	75.9	55.6	76	75.9	73.8	72.3
	2. R.norvegicus_Prx2	98.5		93.4	86.9	76.1	75.6	75.6	76.6	76.1	77.2	76.1	77.7	77.2	76.6	78.2	66.8	74.4	75.9	75.9	55.6	76	76.4	74.3	72.8
	3. H.sapiens_Prx2	93.4	93.4		89.4	77.7	77.2	77.2	78.2	77.7	78.7	76.6	79.2	77.7	76.6	79.2	68.1	75.9	77.4	75.9	55.6	76	76.9	74.3	72.3
	4. B.taurus_Prx2	86.4	86.9	89.4		75.3	75.3	74.7	75.8	74.7	76.8	74.2	76.3	75.3	74.7	79.8	66.1	73	73	74.5	55	75	74.5	73.8	72.3
	5. C.idella_Prx2	76.1	76.1	77.7	75.3		99.5	99.5	99	98	98	98	93.4	94.4	88.3	85.3	77.4	79.3	80.8	81.3	61	83.8	81.3	72.1	73.7
	6. M.piceus_Prx2	75.6	75.6	77.2	75.3	99.5		99	98.5	97.5	97.5	97.5	92.9	94.9	87.8	84.8	77	79.3	80.8	81.3	61	83.8	81.3	72.1	73.7
	7. A.grahami_Prx1	75.6	75.6	77.2	74.7	99.5	99		98.5	98.5	97.5	97.5	92.9	93.9	87.8	84.8	77	79.8	80.3	80.8	61	83.8	80.8	71.6	73.2
	8. R.uyekii_Prx1	76.6	76.6	78.2	75.8	99	98.5	98.5		97.5	97.5	97	92.9	93.4	87.8	85.3	76.5	79.8	81.3	81.8	61.6	84.8	81.3	72.6	74.1
	9. C.carpio_NKEF-B	76.1	76.1	77.7	74.7	98	97.5	98.5	97.5		98	97	92.4	93.4	87.3	84.3	76.5	80.3	80.8	81.3	61	83.8	80.3	71.1	72.7
	10.C.auratus_Prx1	77.2	77.2	78.7	76.8	98	97.5	97.5	97.5	98		97	93.4	94.4	87.3	85.3	76.5	79.8	80.8	81.3	61	83.8	80.3	70.6	72.2
	11.D.rerio_Prx2	76.1	76.1	76.6	74.2	98	97.5	97.5	97	97	97		92.4	93.4	88.3	84.3	77	79.3	80.8	81.8	61.6	84.8	80.8	72.1	73.7
	12.T.fulvidraco_Prx2	77.2	77.7	79.2	76.3	93.4	92.9	92.9	92.9	92.4	93.4	92.4		98	88.3	85.8	75.2	77.8	79.8	78.3	60.4	82.8	79.8	69.7	69.8
	13.I.punctatus_Prx2	76.6	77.2	77.7	75.3	94.4	94.9	93.9	93.4	93.4	94.4	93.4	98		87.3	84.3	75.2	77.8	79.8	79.3	60.4	82.8	79.8	69.2	70.2
	14.L.crocea_Prx1	76.6	76.6	76.6	74.7	88.3	87.8	87.8	87.8	87.3	87.3	88.3	88.3	87.3		89.8	80.1	78.8	80.3	81.3	59.7	83.8	80.3	69.7	69.8
	15.C.semilaevis_Prx2	78.7	78.2	79.2	79.8	85.3	84.8	84.8	85.3	84.3	85.3	84.3	85.8	84.3	89.8		77.4	77.3	78.8	81.8	59.7	82.8	79.3	71.6	70.2
	16.O.latipes_Prx2	67.3	66.8	68.1	66.1	77.4	77	77	76.5	76.5	76.5	77	75.2	75.2	80.1	77.4		67.4	68.7	71.4	48.4	61.7	69.6	61.3	63.2
	17.M.musculus_Prx1	74.4	74.4	75.9	73	79.3	79.3	79.8	79.8	80.3	79.8	79.3	77.8	77.8	78.8	77.3	67.4		95.5	87.4	59.4	81	79.9	68	69.1
	18.H.sapiens_Prx1	75.9	75.9	77.4	73	80.8	80.8	80.3	81.3	80.8	80.8	80.8	79.8	79.8	80.3	78.8	68.7	95.5		88.4	60.6	84	81.4	70	70.5
	19.G.gallus_Prx1	75.9	75.9	75.9	74.5	81.3	81.3	80.8	81.8	81.3	81.3	81.8	78.3	79.3	81.3	81.8	71.4	87.4	88.4		61.9	87	83.9	71.4	71.5
	20.C.carpio_Prx1	55.6	55.6	55.6	55	61	61	61	61.6	61	61	61.6	60.4	60.4	59.7	59.7	48.4	59.4	60.6	61.9		98	66.9	52.5	52.5
	21.C.carpio_Prx1	76	76	76	75	83.8	83.8	83.8	84.8	83.8	83.8	84.8	82.8	82.8	83.8	82.8	61.7	81	84	87	98		94	74	73
	22.D.rerio_Prx1	75.9	76.4	76.9	74.5	81.3	81.3	80.8	81.3	80.3	80.3	80.8	79.8	79.8	80.3	79.3	69.6	79.9	81.4	83.9	66.9	94		71.9	70
	23.X.laevis_Prx2	73.8	74.3	74.3	73.8	72.1	72.1	71.6	72.6	71.1	70.6	72.1	69.7	69.2	69.7	71.6	61.3	68	70	71.4	52.5	74	71.9		90.8
	24.X.tropicalis_Prx2	72.3	72.8	72.3	72.3	73.7	73.7	73.2	74.1	72.7	72.2	73.7	69.8	70.2	69.8	70.2	63.2	69.1	70.5	71.5	52.5	73	70	90.8	

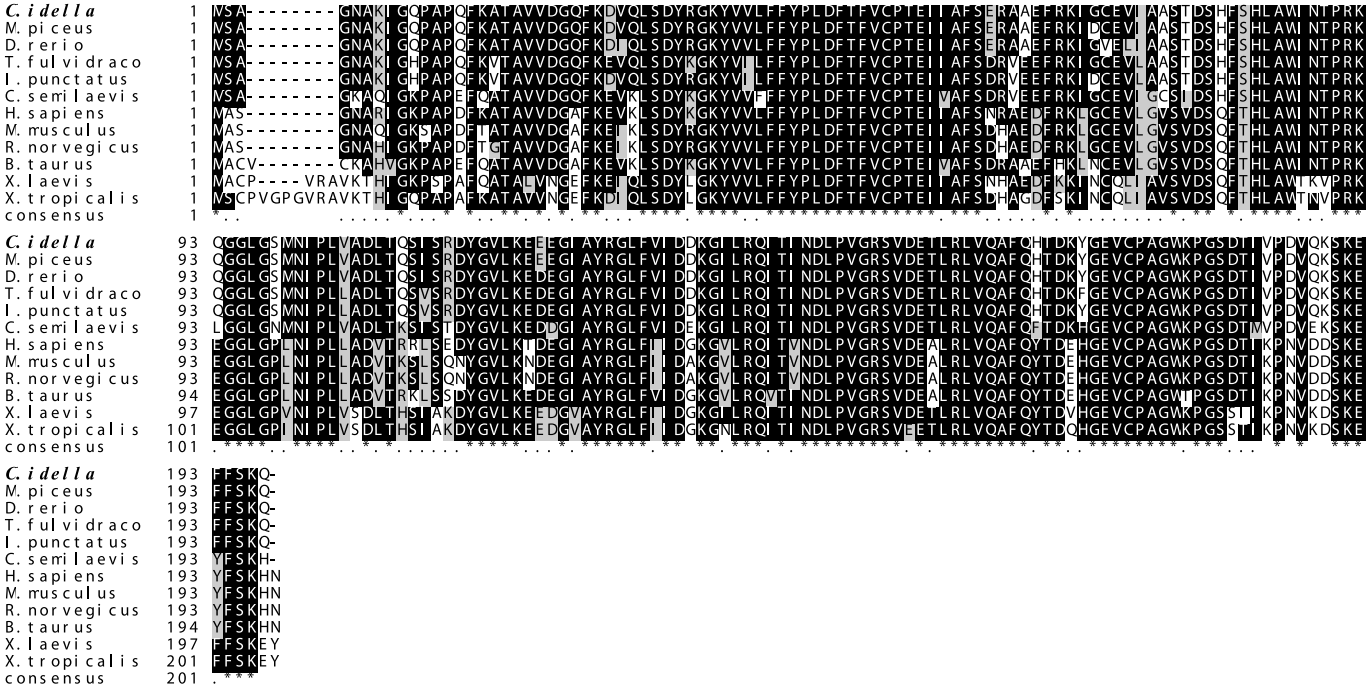

Fig. 2. Multiple alignments of CiPrx2 with the amino acid sequences from other species. TRX-Superfamily signatures FYPLDFTFVCPTEI and GEVCPA are boxed red. The black shade represented 100% identity, dark gray represented 80% identity. Accession numbers are: *Mus musculus* Prx2 (NP 001304314.1), *Rattus norvegicus* Prx2 (NP 058865.1), *Homo sapiens* Prx2 (NP 005800.3), *Bos taurus* Prx2 (NP 777188.1), *Mylopharyngodon piceus* Prx2 (ALD62538.1), *Danio rerio* Prx2 (NP 001002468.1), *Tachysurus fulvidraco* Prx2 (XP 027034897.1), *Ictalurus punctatus* Prx2 (XP 017313378.1), *Cynoglossus semilaevis* Prx2 (XP 008315854.1), *Oryzias latipes* Prx2 (XP 011478972.1), *Xenopus laevis* Prx2 (NP 001085414.1), *Xenopus tropicalis* Prx2 (NP 989001.1).

3. Results and discussion

3.1. Bioinformatics analysis

The full-length cDNA of *CiPrx2* was 1163 bp containing a 5′-UTR of 52 bp, a 3′-UTR of 517 bp with the putative polyadenylation consensus signal (AATAAA), an ORF of 594 bp encoding polypeptides of 197 amino acids with a predicted molecular mass of 21.84 kDa and theoretical isoelectric point of 5.93. The cDNA sequence and the deduced amino acid sequence of CiPrx2 were shown in Fig. 1A. The redoxin (8–157 aa) conserved protein domain was detected in CiPrx2 protein by using SMART (Fig. 1B). No signal peptide was detected by the signalP program.

Multiple alignments of the deduced amino acid sequences showed

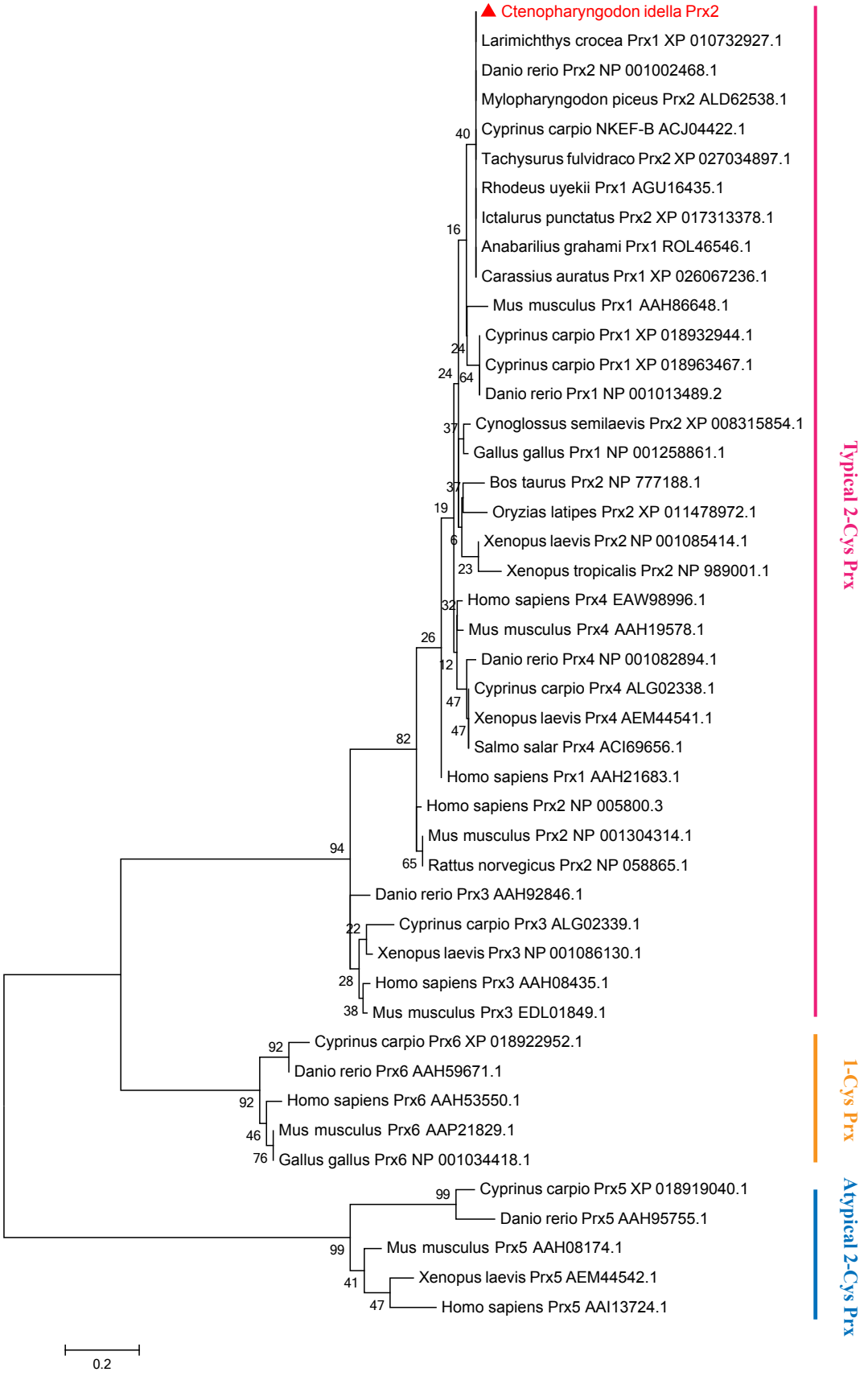

(caption on next page)

Fig. 3. The neighbor-joining phylogenetic tree analyses of CiPrx2 amino acid sequence with the amino acid sequences of other known Prx2 members. The confidence in each node was assessed by 1000 bootstraps. GenBank accession numbers encoding Prxs were as follows: *Homo sapiens* Prx2 (NP 005800.3), *Mus musculus* Prx2 (NP 001304314.1), *Bos taurus* Prx2 (NP 777188.1), *Danio rerio* Prx2 (NP 001002468.1), *Rattus norvegicus* Prx2 (NP 058865.1), *Cyprinus carpio* NKEF-B (ACJ04422.1), *Rhodeus uyekii* Prx1 (AGU16435.1), *Mylopharyngodon piceus* Prx2 (ALD62538.1), *Anabarilius grahami* Prx1 (ROL46546.1), *Larimichthys crocea* Prx1 (XP 010732927.1), *Carassius auratus* Prx1 (XP 026067236.1), *Cynoglossus semilaevis* Prx2 (XP 008315854.1), *Xenopus laevis* Prx2 (NP 001085414.1), *Xenopus tropicalis* Prx2 (NP 989001.1), *Oryzias latipes* Prx2 (XP 011478972.1), *Cyprinus carpio* Prx1 (XP 018963467.1), *Cyprinus carpio* Prx1 (XP 018932944.1), *Ictalurus punctatus* Prx2 (XP 017313378.1), *Tachysurus fulvidraco* Prx2 (XP 027034897.1), *Homo sapiens* Prx1 (AAH21683.1), *Cyprinus carpio* Prx3 (ALG02339.1), *Danio rerio* Prx3 (AAH92846.1), *Homo sapiens* Prx3 (AAH08435.1), *Mus musculus* Prx3 (EDL01849.1), *Xenopus laevis* Prx3 (NP 001086130.1), *Cyprinus carpio* Prx4 (ALG02338.1), *Homo sapiens* Prx4 (EAW98996.1), *Mus musculus* Prx4 (AAH19578.1), *Xenopus laevis* Prx4 (AEM44541.1), *Xenopus laevis* Prx5 (AEM44542.1), *Homo sapiens* Prx5 (AAI13724.1), *Mus musculus* Prx5 (AAH08174.1), *Homo sapiens* Prx6 (AAH53550.1), *Mus musculus* Prx6 (AAP21829.1), *Salmo salar* Prx4 (ACI69656.1), *Danio rerio* Prx4 (NP 001082894.1), *Cyprinus carpio* Prx5 (XP 018919040.1), *Cyprinus carpio* Prx6 (XP 018922952.1), *Gallus gallus* Prx6 (NP 001034418.1), *Gallus gallus* Prx1 (NP 001258861.1), *Danio rerio* Prx1 (NP 001013489.2), *Mus musculus* Prx1 (AAH86648.1), *Danio rerio* Prx5 (AAH95755.1), *Danio rerio* Prx6 (AAH59671.1).

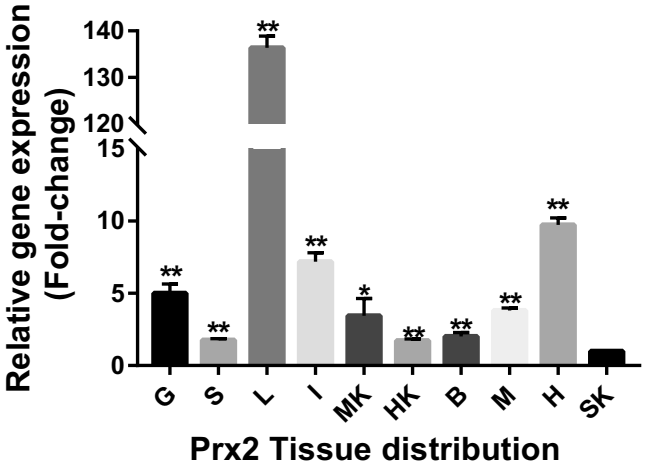

Fig. 4. The constitutive expressions of *CiPrx2* in different tissues of grass carp. The determined tissues included SK: skin; S: spleen; B: brain; G: gill; L: liver; HK: head kidney; H: heart; MK: middle kidney; M: muscle; I: intestine (n = 5). Expression values were normalized to β-actin and the date were shown as mean ± SD of triplicate assays. Expression levels in skin was used as control and set to 1.0. Asterisks (*) representative of significant difference (** = p ≤ 0.01).

that the 2-cys Prx signature motif 1 (FYPLDFTFVCPTEI) and motif 2 (GEVCPA) were conserved in all the analyzed Prx2s. Additionally, the two highly conserved cysteine residue (Cys51 and Cys172) were predicted within the 2-cys Prx signature motifs. The deduced amino acid sequence of CiPrx2 showed high similarity with other Thioredoxin-like superfamilies from many species, especially in the functional area (Table 3 and Fig. 2). The results revealed that the similarity of CiPrx2 was 99.5% with *M. piceus* and *Anabarilius grahami*, 99.0% with *Rhodeus uyekii*, and 98.0% with *C. carpio*, *Carassius auratus* and *Danio rerio*. Thus, Prx2 in grass carp is highly evolutionarily conserved.

To determine the molecular evolutionary relationship, Prx proteins from various vertebrate species were used to construct a phylogenetic tree. As expected, three major clades corresponding to typical 2-Cys Prxs (Prx1-Prx4), 1-Cys Prx (Prx6) and atypical 2-Cys Prxs (Prx5) were observed. In neighbor-joining tree (Fig. 3), Prx1s, Prx2s, Prx3s, Prx4s were clustered together, and then were joined by Prx6s. Prx5s were formed an independent branch. The phylogenetic relationship analysis implied that Prx1, Prx2, Prx3 and Prx4 had a closer evolution position in genetic structure, then Prx6 had a relatively further distance to Prx2 and Prx5. These results confirm that CiPrx2 proteins investigated in this study belong to the typical 2-Cys Prx subfamily.

3.2. Tissue expression analysis of CiPrx2

CiPrx2 mRNA expression levels in 10 tissues showed that it was ubiquitously expressed in all tested tissues, including liver, heart, muscle, spleen, gill, intestine, skin, head kidney, middle kidney and brain. In the present study, the skin was set as the calibrator, that was, the expression level of the *CiPrx2* from the skin was defined as 1.00. The β-actin was used as an internal control. As shown in Fig. 4, the expression level varied among different tissues. The highest expression of the *CiPrx2* transcript was detected in liver (136.36-fold), then heart (9.74-fold), gill (5.01-fold) and intestine (7.20-fold) following. The relative low expression was noted in skin (Fig. 4).

3.3. Temporal expression profiles of CiPrx2 after GCRV infection

To test the effectiveness of GCRV infection, the relative copy number of the virus in gill were examined by RT-qPCR (special primers in Table 1). The relative copy number of GCRV on day 1 after infection were used as a reference for normalization. As shown in Fig. 5A, the relative copy number of GCRV were raised slowly in the first three days after infection, and then increased rapidly in the next 4 days and

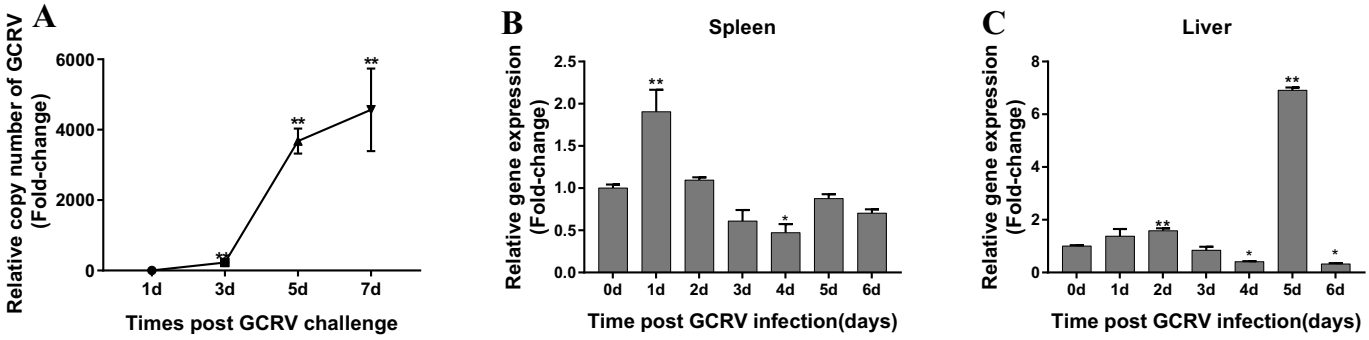

Fig. 5. (A) A relative number of GCRV copies in gill. The relative copy number of GCRV on day 1 after infection were used as a reference for normalization. The β-actin was used as an internal control. (B–C) Expression analysis of *CiPrx2* after GCRV infection. The mRNA expression patterns of Prx2 in spleen (B) and liver (C) under GCRV infection were detected by RT-qPCR at 0–6 dpi. Expression levels on day 0 was used as control and set to 1.0. The β-actin was used as an internal control. All data were given in terms of relative mRNA expression as means ± SD (n = 5). Asterisks (*) representative of significant difference (* = p ≤ 0.05, ** = p ≤ 0.01).

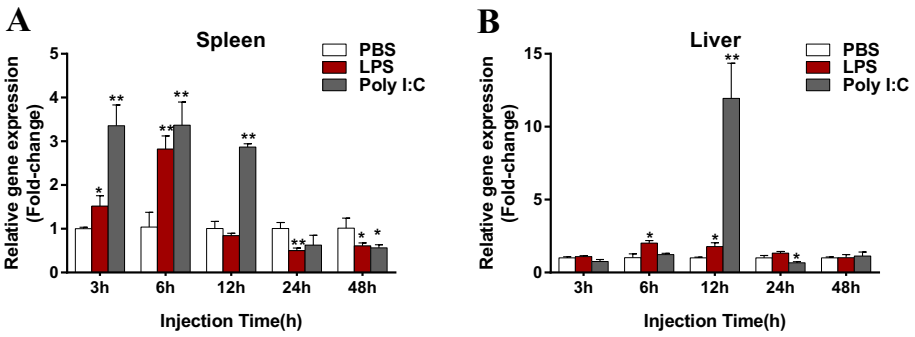

Fig. 6. Expression analysis of *CiPrx2* under stimulation of LPS and poly I:C. The mRNA expression patterns of *CiPrx2* in fish spleen (A) and liver (B) under stimulation of LPS and poly I:C as well as the control group treated with PBS were detected by quantitative real-time PCR at 0, 3, 6, 12, 24 and 48 h post-injection. The β-actin was used as an internal control. All data were given in terms of relative mRNA expression as means ± SD (n = 5). Asterisks (*) representative of significant difference (* = $p \leq 0.05$, ** = $p \leq 0.01$).

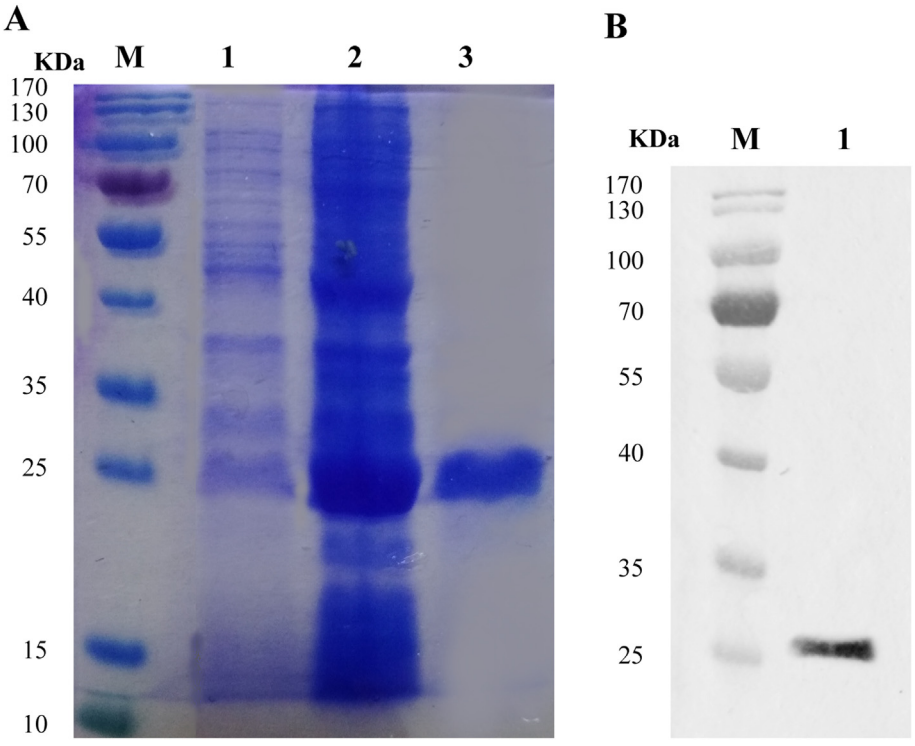

Fig. 7. (A) Sodium dodecyl sulfate-polyacrylamide gel electrophoresis (SDS-PAGE) analysis of Prx2 recombinant protein. Lane M: Protein molecular weight marker; Lane 1: before IPTG induction; Lane 2: after 6 h induction with 1.0 mM IPTG; Line 3, Purified recombinant Prx2 protein. (B) Western blot analysis of recombinant proteins in the *E. coli* BL21 (transsetta DE3) cells with anti-His-tag antibody. Lane M: Protein molecular weight marker; Lane 1: Purified recombinant Prx2 protein.

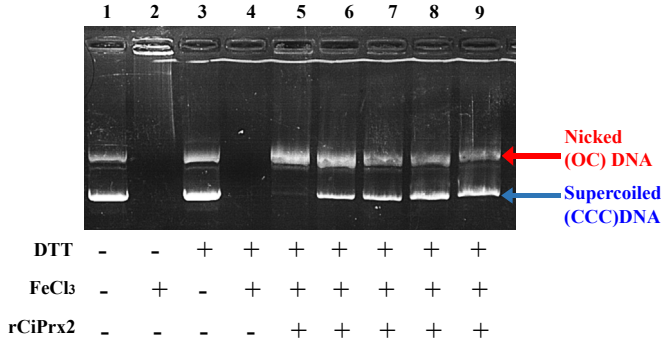

Fig. 8. Determination of rCiPrx2 protected supercoiled DNA cleavage in mixed-function oxidase (MFO) assay. 1: pEGFP-N3 without incubation; 2: pEGFP-N3 + $FeCl_3$ (10 μM); 3: pEGFP-N3 + DTT (10 mM); 4: pEGFP-N3 + MFO mix (10 μM $FeCl_3$ + 10 mM DTT); 5: pEGFP-N3 + MFO mix + 1 μg of rCiPrx2; 6: pEGFP-N3 + MFO mix + 4 μg of rCiPrx2; 7: pEGFP-N3 + MFO mix + 8 μg of rCiPrx2; 8: pEGFP-N3 + MFO mix + 16 μg of rCiPrx2; 9: pEGFP-N3 + MFO mix + 24 μg of rCiPrx2. OC DNA: open circular plasmid DNA; CCC: covalently closed circular DNA.

reached the peak on 7 dpi, which showed that GCRV infection had occurred.

To determine the effects of viral infection on *CiPrx2* gene expression in the innate immune system, the levels of *CiPrx2* mRNA transcripts in liver and spleen were examined. In the spleen, the levels of *CiPrx2* mRNA transcripts were increased sharply and reached the peak (1.91-fold) on 1 dpi, and then declined slowly and dropped to the lowest level on 4 dpi (0.47-fold). Subsequently, the expression levels almost reached the basal level (Fig. 5B). In the liver, the *CiPrx2* expression levels were slowly up-regulated in the first two days, followed by a decline at 3 and 4 dpi, then increased sharply on 5 dpi (6.90-fold), finally declined on 6 dpi (Fig. 5C).

3.4. Transcription analysis of CiPrx2 after PAMPs challenge

To preliminary explore whether the *CiPrx2* expression was affected by PAMPs infection, the expression profiles of *CiPrx2* in spleen and liver were analyzed by RT-qPCR (Fig. 6). As the results show, LPS and poly I:C stresses could induce the expression level of *CiPrx2* in spleen (Fig. 6A) and liver (Fig. 6B). However, the expression patterns of *CiPrx2* had some difference under different stresses treatments or in various tissues. In spleen, the levels of *CiPrx2* mRNA transcripts gradually increased after LPS challenge, and reached peak values with a 2.82-fold

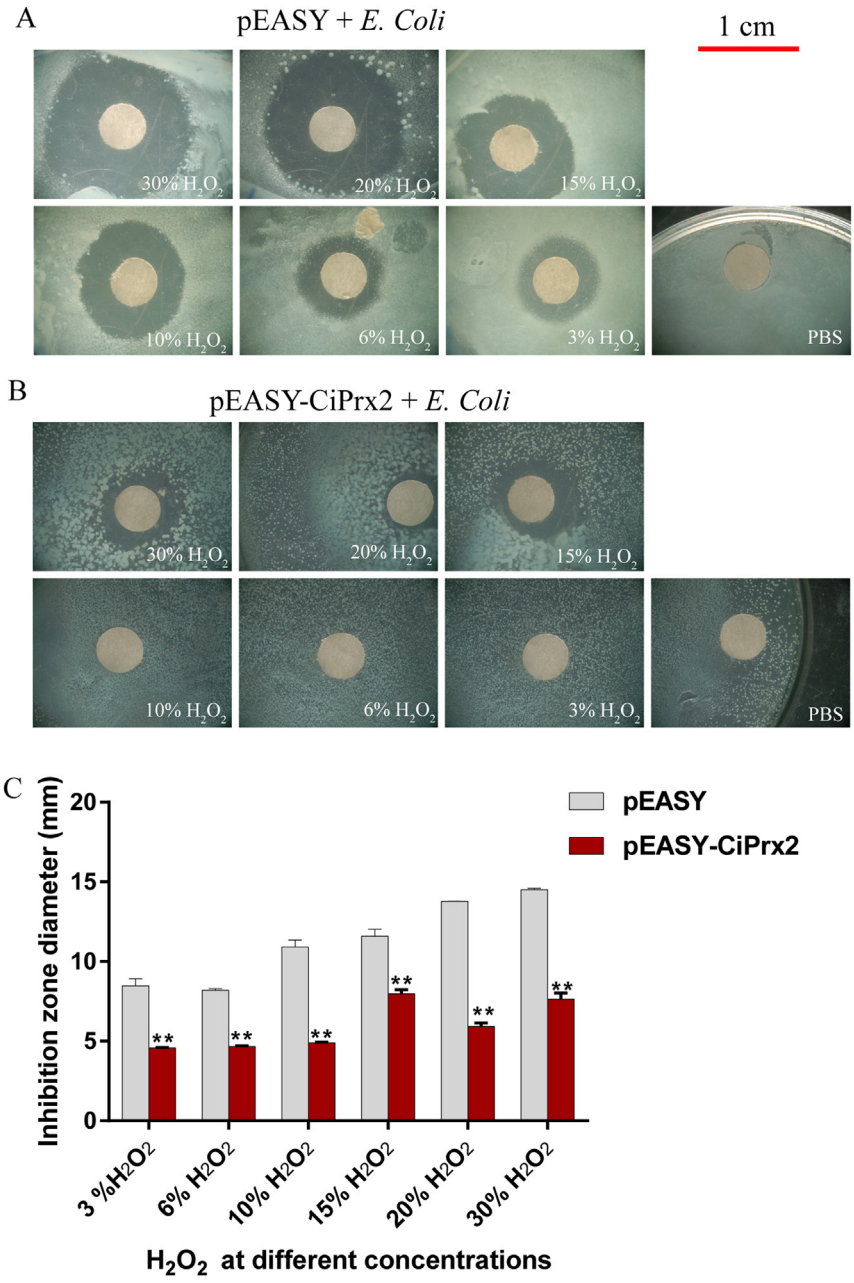

Fig. 9. In vivo antioxidant activity assay using *E. coli* cells overexpressing CiPrx2. (A) Bacteria transfected with only pESAY vector were used as the negative controls; (B) LA agar plates (LB with ampicillin) were inoculated with *E. coli* cells harboring a plasmid DNA for CiPrx2 overexpression; Filter discs treated with different concentrations of H_2O_2, including the concentration of H_2O_2 at 30%, 20%, 15%, 10%, 6%, 3%. (C) Inhibition zone diameter of *E. coli* after H_2O_2 challenge. Data was showed as mean ± SD (n = 3). Error bars above the vertical bars indicated statistically significant differences between every intergroup by the asterisk (**P ≤ 0.01).

increase compared to the control group at 6 hpi, then rapidly declined at 12 hpi. After poly I:C challenge, the *CiPrx2* expression reached rapidly peak values at 6 hpi (3.36-fold), then gradually declined gradually dropped to a relatively lower level at 48 hpi (0.56-fold). In liver, the *CiPrx2* transcript gradually increased as time went by and peaked at 12 h (11.94-fold) after poly I:C challenge. After LPS challenge, the levels of *CiPrx2* mRNA transcripts were dramatically up-regulated at 6 and 12 hpi and then almost reached the basal level. In general, the temporal expression pattern of *CiPrx2* had a rising trend after PAMPs challenge.

3.5. Expression, purification, and western blotting of recombinant CiPrx2

The recombinant plasmid pEASY-CiPrx2 was transformed into *E. coli* BL21 and then expressed by induction with IPTG. After IPTG induction for 6 h, the whole cell lysate of the positive clone was obtained. Then, the rCiPrx2-6 × His tagged fusion protein was separated by SDS-PAGE, and an obvious band with a molecular weight of approximately 25 kDa was detected (Fig. 7A), which is consistent with the predicted molecular mass of rCiPrx2 with the His-tag added by the vector. When the rCiPrx2 was purified by the Ni-NTA resin, Western blot analysis showed only one specific target protein with a molecular weight of 25 kDa (Fig. 7B). From the above results, CiPrx2 recombinant expression and purification were successfully performed. The purified protein was used in the next experiments.

3.6. DNA protection assay through antioxidant property of CiPrx2

To investigate whether the recombinant rCiPrx2 can prevent DNA from damage caused by the ROS generated from a MFO system, the DNA protection assay was performed. The pEGFP-N3 plasmid was incubated with rCiPrx2 protein in MFO system and DNA damage was analyzed by electrophoresis. The MFO system generated using DTT and $FeCl_3$, was able to induce damages to pEGFP-N3 plasmid converting a covalently closed circular DNA (CCC DNA) to the nicked form (OC DNA). The results revealed that the rCiPrx2 protein inhibited DNA

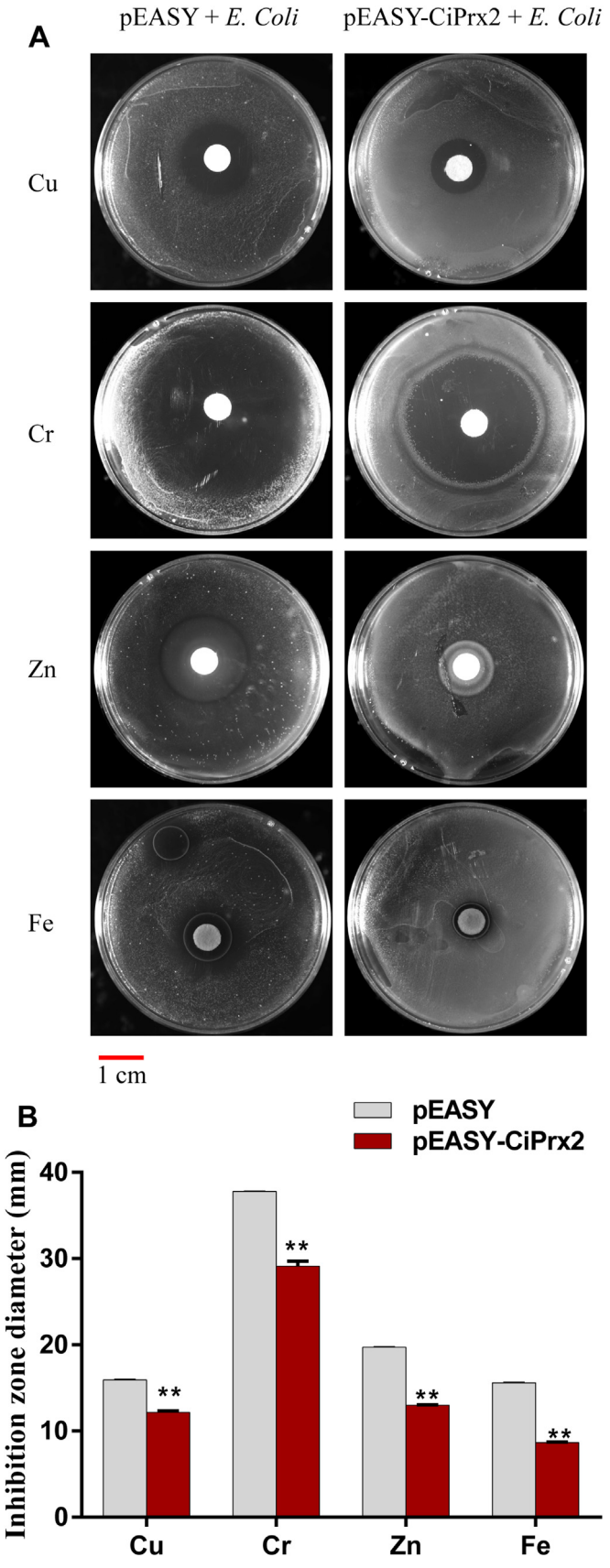

Fig. 10. Metal stress resistance properties assays of CiPrx2 from *E. coli* in vitro. (A) *E. coli* with pEASY-CiPrx2 as the experimental group and only pEASY as control group under 1 mol/l heavy metal stimulation; (B) Inhibition zone diameter of *E. coli* after 1 mol/l heavy metal challenge; Data was showed as mean ± SD (n = 3). Error bars above the vertical bars indicated statistically significant differences between every intergroup by the asterisk

damage in dose-dependent manner compared with the control (Fig. 8). Furthermore, the rCiPrx2 protein had the ability to inhibit DNA damage even at lower concentrations, but the level of protection was positively correlated with the concentration of rCiPrx2 protein.

3.7. H_2O_2 and heavy metal toxicity stress resistance properties assays in vitro

E. coli BL21 cells strains transformed with pEASY-CiPrx2 vector or pEASY-Blunt empty vector were cultured agarose plates with ampicillin, then H_2O_2 and heavy metal toxicity stress resistance properties of CiPrx2 were tested in *vitro*. Under each concentration of H_2O_2 and different kinds of heavy metals, the growth of the control strains transformed with pEASY-Blunt empty vector was significantly inhibited compared with the experimental strains transformed with pEASY-CiPrx2 vector. As shown in Fig. 9, the zone inhibition diameters were increased as the increase of concentration of H_2O_2. Moreover, the clearing zone diameters of DE3-pEASY-CiPrx2 were significantly smaller than the control groups, and the values of diameter were 0.54, 0.57, 0.44, 0.68, 0.42 and 0.53-fold of the control group under the stimulation of H_2O_2 at a concentration of 30%, 20%, 15%, 10%, 6%, 3%, respectively. Under heavy metal stress, the clearing zone diameters of DE3-pEASY-CiPrx2 were markedly smaller than control groups; values were extremely significantly declined to 0.76, 0.77, 0.66 and 0.55-fold of control groups under $CuSO_4{\cdot}5H_2O$, $K_2Cr_2O_7$, $FeCl_3{\cdot}6H_2O$ and $ZnSO4{\cdot}7H_2O$ at a concentration of 1 mol/L (Fig. 10). The above experimental results show that CiPrx2 protein can protect *E. coli* BL21 from H_2O_2 and heavy metal toxicity stress to some extent.

3.8. Subcellular localization of CiPrx2

To determine the subcellular localization of CiPrx2, the ORF of CiPrx2 was constructed into the pEGFP-N3 expression vector and then fluorescence was observed at 24 h post-transfection. The results revealed that the CiPrx2-GFP fusion protein were only distributed in the cytoplasm, but the control pEGFP-N3 was strongly distributed uniformly throughout the entire cell including the nucleus (Fig. 11A). Confirmation of the expression of CiPrx2-GFP fusion protein was performed by Western blotting analysis, and the recombinant CiPrx2-GFP showed correct molecular weight as revealed with GFP-Tag antibody (Fig. 11B).

4. Discussion

Peroxidase proteins play an important role in protecting organisms from oxidative stress [12], which are identified in various organisms ranging from prokaryotes to eukaryotes. In addition, there is increasing evidence that they are involved in immune response after microbial infection [35]. In this study, a novel Prx2 gene was firstly isolated and characterized from *C. idella* (*CiPrx2*), containing ORF of 594 bp, encoding polypeptides of 197 amino acids. By analyzing the deduced amino acid sequence and multiple alignments, the two highly conserved cysteines (Cys51 and Cys172) were existed in the Prx signature motifs FYPLDFTFVCPTEI and GEVCPA, respectively, which are very conserved in mammals, fish, fungi and plants [12,36]. Both conserved Cys residues are required for their catalytic function, which means that Prx2 could act as a reductant to reduce the ROS produced during cell metabolism and oxidative stress [37]. The sequences GGLG and YF or FF were only detected in eukaryotic 2-Cys Prxs proteins and contributed to the regulatory activity for H_2O_2-mediated signal transduction [38]. A consensus sequence (TPRK) for phosphorylation by cyclin-dependent kinases [39] was also found in CiPrx2. The deduced amino acid sequence showed high similarity to previously reported Prxs from other fish and 99.5% similarity with *M. piceus* and *A. graham,* 99.0% with *R. uyekii,* and 98.0% with *C. carpio*, *C. auratus* and *D. rerio*. From phylogenetic tree analysis, Prxs can be classified into three classes (typical 2-

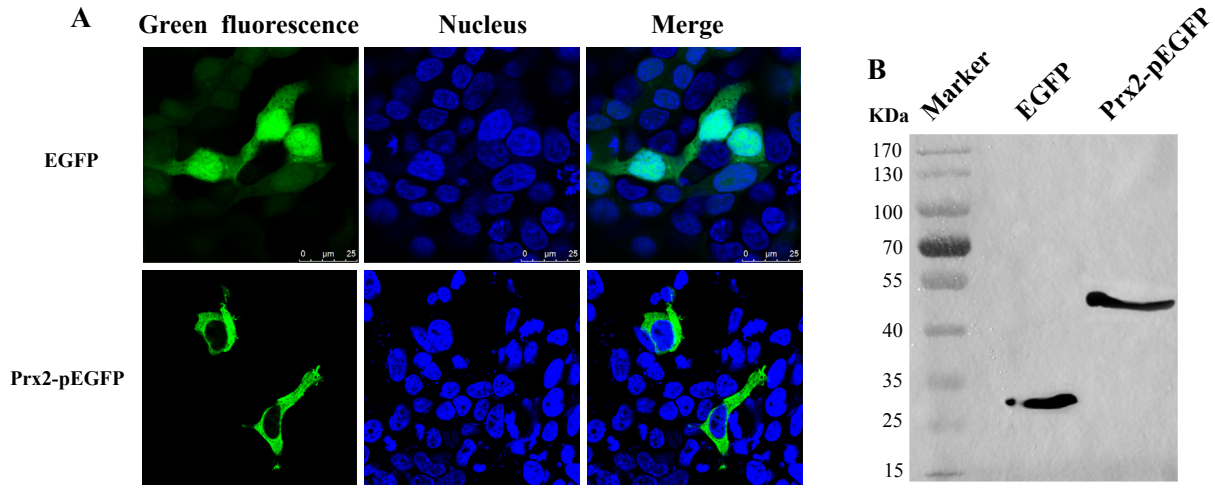

Fig. 11. Subcellular localization of CiPrx2 proteins in HEK 293T cells. (A) HEK 293T cells were transiently transfected with pEGFP-N3, pEGFP-N3-CiPrx2, respectively. At 24h post-transfection, the nucleus was stained with Hoechst 33342 and the cells were detected and photographed under a confocal microscope (scale bar, 25 μm). (B) The expression of GFP fusion proteins were confirmed by Western blotting analysis using anti-GFP antibody.

Cys, atypical 2-Cys and 1-Cys) or six subfamilies (Prx1-6). Prx2 was more similar to Prx1, 3, 4, and far from Prx5 and Prx6. All these characters indicated that Prx1-4 were member of typical 2-Cys Prx, and Prx5 was atypical 2-Cys member of Prxs while Prx6 was the member of 1-Cys (Figs. 1–3) [40–44].

These Prxs isoforms also differ in their cellular distributions [45]. Prx1, 2 and 6 are localized in the cytosol whereas Prx3 exists in the mitochondria and Prx4 has an N-terminal signal peptide targeting it for secretion from the cell. Prx5 is localized intracellularly to the cytosol, mitochondria, nuclei and peroxisomes [46]. SignaIP 4.1 analysis showed that the amino acid sequence of CiPrx2 was lacked the signal peptide, which indicated that CiPrx2 may be an intracellular protein. Subcellular localization results indicate that CiPrx2 was a cytoplasmic protein (Fig. 11). So, the subcellular localization of CiPrx2 protein was consistent with previous data.

The tissue expression analysis shown that *CiPrx2* was constitutively expressed in all examined tissues with different expression levels. The results indicated that *CiPrx2* was a ubiquitously expressed gene and could potentially play diverse roles in different physiological processes. The highest expression of the *CiPrx2* was detected in liver (136.36-fold), then heart (9.74-fold), gill (5.01-fold) and intestine (7.20-fold) following (Fig. 4). Ren and his group reported that *M. miiuy* Prx2 mRNA was highly expressed in the fin, liver, heart, and intestine, which are involved in the immune response against pathogens [44]. However, in *C. carpio*, the highest mRNA level of Prx2 in kidney, followed by in head kidney, blood cells, liver, spleen and muscle [19], which might indicate the different roles of Prx2 in various fish species. The liver was closely related to immune response, it is known to home to innate immune cells (monocytes, NK and NKT cells) that can identify and clear pathogens, and many of inflammation cell factors are synthesized in the liver [47,48], so the high expression of Prx2 in the liver implied its immune function. The heart is the center of circulation system, the main source of cardiac energy is material oxidation and will produce free radicals, the expression of Prx2 can protect myocardial cell from free radical, and so it is in other tissues. The gill, directly exposed to the external environment and constantly contact with pathogens and environmental toxicities, is one of the mucosal barriers in fish exerting an important role in mucosal immune response [49]. The spleen is the primary secondary lymphoid organ in fish [50]. In summary, the high expressions of *CiPrx2* in immune-related tissues suggested that it plays critically important roles in the immune system of grass carp.

Biotic and abiotic stress frequently affect the survival of aquatic animals, such as bacterial and viral infections, heavy metal pollution and salinity fluctuation, leading to increased ROS production [51–55]. It is well known that liver and spleen are important immune organs, playing an important role in immune response [47,48,50]. Therefore, in order to initially investigate whether *CiPrx2* was regulated in response to these stresses, the expression profile of *CiPrx2* gene was analyzed in liver and spleen following the infection of GCRV, poly I:C and LPS. After GCRV challenge, the maximum transcript level of *CiPrx2* was observed on 1 dpi in spleen and 5 dpi in liver. In addition, the expression level of *CiPrx2* was significantly induced under poly I:C and LPS stimulation in spleen and liver. Some studies have shown that Prx2 has important functions in immune response. In pufferfish, stimulation with LPS inhibited Prx2 gene expression in most tissues but enhanced Prx2 transcriptions in spleen [21]. In black carp, the expression levels of MpPrx2 mRNA in the liver were up-regulated after LPS challenge [25]. After infected with SVCV, the expression level of *C. carpio* Prx2 was significantly increased in blood cells, gill, muscle, intestine and spleen, but maintained in liver, and decreased significantly in kidney and head kidney [19]. Following the infection of *Vibrio anguillarum*, the relative expression quantity of *M. miiuy* Prx2 in the liver at 6 h after infection was 3.9 times to control level, a higher expression level at 24 h after injection in the spleen [44]. These results collectively indicate that Prx2 function differently among various species as well as under different PAMPs stimulation.

In this paper, the recombinant rCiPrx2 protein was expressed in *E. coli* BL21. CiPrx2 protein was purified using Ni-NTA affinity chromatography and detected via SDS-PAGE. Mouse polyclonal antibody was used to detect purified CiPrx2 protein, which showed a molecular mass of approximately 25 kDa that was specific to the His-Tag HRP polyclonal antibody. Subsequently, DNA protecting activity of rAjPrdx6 in oxidative damage was determined using MFO assay [56]. The MFO system can generate ROS [57] including superoxides, hydroxyl radicals and hydrogen peroxides by metal catalyzed Fenton reactions [58]. Therefore, presence of the MFO system can induce the nicking of supercoiled plasmid DNA into open circular form and leads to the sever DNA damage [56,58]. Prxs are thought to have a role in the inhibition of DNA damage caused by ROS [59]. In this study, the rCiPrx2 protein inhibited DNA damage in dose-dependent manner compared with the control, and the similar results have also been reported [60–63]. H_2O_2 and heavy metal toxicity stress resistance assays of CiPrx2 protein were performed in *E. coli* BL21, which is a useful model for oxidative stress studies at the cellular level [64]. Combined with the above experiments, the results showed that CiPrx2 protein could protect *E. coli* BL21 from H_2O_2 and heavy metal toxicity stress to some extent, which was consistent with previous studies [34,65].

In summary, the molecular cloning and characterization of a Prx2

homologue (*CiPrx2*) were described from grass carp and it ubiquitously expressed in the various tissues, such as liver, heart, gill and intestine. The temporal expression profiles of *CiPrx2* gene were analyzed in liver and spleen infected with GCRV, poly I:C and LPS, which showed that *CiPrx2* was likely to be involved in the immune response against viral and bacterial infection. Subcellular localization results showed that CiPrx2-GFP fusion protein was only distributed in the cytoplasm. The purified recombinant CiPrx2 possessed apparent antioxidant activity and could protect DNA against oxidative damage. Finally, CiPrx2 protein could obviously inhibit heavy metal and H_2O_2 toxicity. However, further researches are needed to better understand the regulation of CiPrx2 under oxidative stresses.

Acknowledgments

This study was supported by the National Natural Science Foundation of China (grant numbers 31721005 and 31572614).

References

[1] C. Bogdan, M. Rollinghoff, A. Diefenbach, Reactive oxygen and reactive nitrogen intermediates in innate and specific immunity, Curr. Opin. Immunol. 12 (1) (2000) 64–76.
[2] V.J. Thannickal, B.L. Fanburg, Reactive oxygen species in cell signaling, Am. J. Physiol. Lung Cell Mol. Physiol. 279 (6) (2000) L1005–L1028.
[3] H. Kamata, H. Hirata, Redox regulation of cellular signalling, Cell. Signal. 11 (1) (1999) 1–14.
[4] J. Nordberg, E.S. Arner, Reactive oxygen species, antioxidants, and the mammalian thioredoxin system, Free Radic. Biol. Med. 31 (11) (2001) 1287–1312.
[5] E.R. Stadtman, R.L. Levine, Protein oxidation, Ann. N. Y. Acad. Sci. 899 (2000) 191–208.
[6] Z.W. Ye, J. Zhang, D.M. Townsend, K.D. Tew, Oxidative stress, redox regulation and diseases of cellular differentiation, Biochim. Biophys. Acta 1850 (8) (2015) 1607–1621.
[7] S. Yla-Herttuala, Oxidized LDL and atherogenesis, Ann. N. Y. Acad. Sci. 874 (1999) 134–137.
[8] E. Cadenas, K.J. Davies, Mitochondrial free radical generation, oxidative stress, and aging, Free Radic. Biol. Med. 29 (3–4) (2000) 222–230.
[9] G. Ermak, K.J. Davies, Calcium and oxidative stress: from cell signaling to cell death, Mol. Immunol. 38 (10) (2002) 713–721.
[10] B.P. Yu, Cellular defenses against damage from reactive oxygen species, Physiol. Rev. 74 (1) (1994) 139–162.
[11] J. Perez-Sanchez, A. Bermejo-Nogales, J.A. Calduch-Giner, S. Kaushik, A. Sitja-Bobadilla, Molecular characterization and expression analysis of six peroxiredoxin paralogous genes in gilthead sea bream (Sparus aurata): insights from fish exposed to dietary, pathogen and confinement stressors, Fish Shellfish Immunol. 31 (2) (2011) 294–302.
[12] H.Z. Chae, S.J. Chung, S.G. Rhee, Thioredoxin-dependent peroxide reductase from yeast, J. Biol. Chem. 269 (44) (1994) 27670–27678.
[13] T.H. Lee, S.L. Yu, S.U. Kim, K.K. Lee, S.G. Rhee, D.Y. Yu, Characterization of mouse peroxiredoxin I genomic DNA and its expression, Gene 239 (2) (1999) 243–250.
[14] M.F. Sanchez-Font, J. Sebastia, C. Sanfeliu, R. Cristofol, G. Marfany, R. Gonzalez-Duarte, Peroxiredoxin 2 (PRDX2), an antioxidant enzyme, is under-expressed in Down syndrome fetal brains, Cell. Mol. Life Sci. CMLS 60 (7) (2003) 1513–1523.
[15] E. Schroder, J.A. Littlechild, A.A. Lebedev, N. Errington, A.A. Vagin, M.N. Isupov, Crystal structure of decameric 2-Cys peroxiredoxin from human erythrocytes at 1.7 A resolution, Structure 8 (6) (2000) 605–615.
[16] T. Yamamoto, Y. Matsui, S. Natori, M. Obinata, Cloning of a housekeeping-type gene (MER5) preferentially expressed in murine erythroleukemia cells, Gene 80 (2) (1989) 337–343.
[17] M.T. Prosperi, D. Ferbus, I. Karczinski, G. Goubin, A human cDNA corresponding to a gene overexpressed during cell proliferation encodes a product sharing homology with amoebic and bacterial proteins, J. Biol. Chem. 268 (15) (1993) 11050–11056.
[18] R. Geiben-Lynn, M. Kursar, N.V. Brown, M.M. Addo, H. Shau, J. Lieberman, A.D. Luster, B.D. Walker, HIV-1 antiviral activity of recombinant natural killer cell enhancing factors, NKEF-A and NKEF-B, members of the peroxiredoxin family, J. Biol. Chem. 278 (3) (2003) 1569–1574.
[19] R. Huang, L.Y. Gao, Y.P. Wang, W. Hu, Q.L. Guo, Structure, organization and expression of common carp (Cyprinus carpio L.) NKEF-B gene, Fish Shellfish Immunol. 26 (2) (2009) 220–229.
[20] D.H. Shin, K. Fujiki, M. Nakao, T. Yano, Organization of the NKEF gene and its expression in the common carp (Cyprinus carpio), Dev. Comp. Immunol. 25 (7) (2001) 597–606.
[21] W.R. Dong, L.X. Xiang, J.Z. Shao, Cloning and characterisation of two natural killer enhancing factor genes (NKEF-A and NKEF-B) in pufferfish, Tetraodon nigroviridis, Fish Shellfish Immunol. 22 (1–2) (2007) 1–15.
[22] D.L. Sutton, G.H. Loo, R.I. Menz, K.A. Schuller, Cloning and functional characterization of a typical 2-Cys peroxiredoxin from southern bluefin tuna (Thunnus maccoyii), Comp. Biochem. Physiol. B Biochem. Mol. Biol. 156 (2) (2010) 97–106.
[23] L. Ren, T. Xu, R. Wang, Y. Sun, Miiuy croaker (Miichthys miiuy) Peroxiredoxin2: molecular characterization, genomic structure and immune response against bacterial infection, Fish Shellfish Immunol. 34 (2) (2013) 556–563.
[24] L. Ren, Y. Sun, R. Wang, T. Xu, Gene structure, immune response and evolution: comparative analysis of three 2-Cys peroxiredoxin members of miiuy croaker, Miichthys miiuy, Fish Shellfish Immunol. 36 (2) (2014) 409–416.
[25] C. Wu, J. Gao, F. Cao, Z. Lu, L. Chen, J. Ye, Molecular cloning, characterization and mRNA expression of six peroxiredoxins from Black carp Mylopharyngodon piceus in response to lipopolysaccharide challenge or dietary carbohydrate, Fish Shellfish Immunol. 50 (2016) 210–222.
[26] D. Zhu, R. Huang, L. Chen, P. Fu, L. Luo, L. He, Y. Li, L. Liao, Z. Zhu, Y. Wang, Cloning and characterization of the LEF/TCF gene family in grass carp (*Ctenopharyngodon idella*) and their expression profiles in response to grass carp reovirus infection, Fish Shellfish Immunol. 86 (2019) 335–346.
[27] D. Zhu, R. Huang, P. Fu, L. Chen, L. Luo, P. Chu, L. He, Y. Li, L. Liao, Z. Zhu, Y. Wang, Investigating the role of BATF3 in grass carp (*Ctenopharyngodon idella*) immune modulation: a fundamental functional analysis, Int. J. Mol. Sci. 20 (7) (2019) 1687.
[28] Y. Wang, Y. Lu, Y. Zhang, Z. Ning, Y. Li, Q. Zhao, H. Lu, R. Huang, X. Xia, Q. Feng, X. Liang, K. Liu, L. Zhang, T. Lu, T. Huang, D. Fan, Q. Weng, C. Zhu, Y. Lu, W. Li, Z. Wen, C. Zhou, Q. Tian, X. Kang, M. Shi, W. Zhang, S. Jang, F. Du, S. He, L. Liao, Y. Li, B. Gui, H. He, Z. Ning, C. Yang, L. He, L. Luo, R. Yang, Q. Luo, X. Liu, S. Li, W. Huang, L. Xiao, H. Lin, B. Han, Z. Zhu, The draft genome of the grass carp (Ctenopharyngodon idellus) provides insights into its evolution and vegetarian adaptation, Nat. Genet. 47 (6) (2015) 625–631.
[29] I. Letunic, T. Doerks, P. Bork, SMART: recent updates, new developments and status in 2015, Nucleic Acids Res. 43 (2015) D257–D260 Database issue.
[30] K. Tamura, D. Peterson, N. Peterson, G. Stecher, M. Nei, S. Kumar, MEGA5: molecular evolutionary genetics analysis using maximum likelihood, Evol. Distance Max. Parsim. Methods, Mol. Biol, Evol. 28 (10) (2011) 2731–2739.
[31] P. Chu, L. He, D. Zhu, L. Chen, R. Huang, L. Liao, Y. Li, Z. Zhu, Y. Wang, Identification, characterisation and preliminary functional analysis of IRAK-M in grass carp (*Ctenopharyngodon idella*), Fish Shellfish Immunol. 84 (2019) 312–321.
[32] K.J. Livak, T.D. Schmittgen, Analysis of relative gene expression data using real-time quantitative PCR and the 2(T)(-Delta Delta C) method, Methods 25 (4) (2001) 402–408.
[33] D. Zhu, Y. Li, R. Huang, L. Luo, L. Chen, P. Fu, L. He, Y. Li, L. Liao, Z. Zhu, Y. Wang, Molecular characterization and functional activity of Prx1 in grass carp (*Ctenopharyngodon idella*), Fish Shellfish Immunol. 90 (2019) 395–403.
[34] R. Bu, L. Yan, C. Zhao, P. Wang, S. Fan, S. Wang, L. Qiu, The acute stresses role of the atypical 2-cys peroxiredoxin PmPrx5 in black tiger shrimp (Penaeus monodon) from biological immunity and environmental toxicity stress, Fish Shellfish Immunol. 81 (2018) 189–203.
[35] T. Ishii, E. Warabi, T. Yanagawa, Novel roles of peroxiredoxins in inflammation, cancer and innate immunity, J. Clin. Biochem. Nutr. 50 (2) (2012) 91–105.
[36] B. Hofmann, H.J. Hecht, L. Flohe, Peroxiredoxins, Biol Chem 383 (3–4) (2002) 347–364.
[37] Z.A. Wood, E. Schroder, J. Robin Harris, L.B. Poole, Structure, mechanism and regulation of peroxiredoxins, Trends Biochem. Sci. 28 (1) (2003) 32–40.
[38] A. Hall, P.A. Karplus, L.B. Poole, Typical 2-Cys peroxiredoxins–structures, mechanisms and functions, FEBS J. 276 (9) (2009) 2469–2477.
[39] J.M. Mates, C. Perez-Gomez, I. Nunez de Castro, Antioxidant enzymes and human diseases, Clin. Biochem. 32 (8) (1999) 595–603.
[40] A. Matsumoto, A. Okado, T. Fujii, J. Fujii, M. Egashira, N. Niikawa, N. Taniguchi, Cloning of the peroxiredoxin gene family in rats and characterization of the fourth member, FEBS Lett. 443 (3) (1999) 246–250.
[41] W. Song, C. Mu, R. Li, C. Wang, Peroxiredoxin 1 from cuttlefish (Sepiella maindroni): molecular characterization of development and its immune response against Vibrio alginolyticus, Fish Shellfish Immunol. 67 (2017) 596–603.
[42] D.-D. Tu, Y.-L. Zhou, W.-B. Gu, Q.-H. Zhu, B.-P. Xu, Z.-K. Zhou, Z.-P. Liu, C. Wang, Y.-Y. Chen, M.-A. Shu, Identification and characterization of six peroxiredoxin transcripts from mud crab Scylla paramamosain: the first evidence of peroxiredoxin gene family in crustacean and their expression profiles under biotic and abiotic stresses, Mol. Immunol. 93 (2018) 223–235.
[43] Y.Z. Yang, Y. Zhao, L. Yang, L.P. Yu, H. Wang, X.S. Ji, Characterization of 2-Cys peroxiredoxin 3 and 4 in common carp and the immune response against bacterial infection, Comp. Biochem. Physiol. B Biochem. Mol. Biol. 217 (2018) 60–69.
[44] L. Ren, T. Xu, R. Wang, Y. Sun, Miiuy croaker (Miichthys miiuy) Peroxiredoxin2: molecular characterization, genomic structure and immune response against bacterial infection, Fish Shellfish Immunol. 34 (2) (2013) 556–563.
[45] D.R. Ambruso, Peroxiredoxin-6 and NADPH oxidase activity, Methods Enzymol. 527 (2013) 145–167.
[46] G.Q. Shi, Z. Zhang, K.L. Jia, K. Zhang, D.X. An, G. Wang, B.L. Zhang, H.N. Yin, Characterization and expression analysis of peroxiredoxin family genes from the silkworm Bombyx mori in response to phoxim and chlorpyrifos, Pestic. Biochem. Physiol. 114 (2014) 24–31.
[47] U. Protzer, M.K. Maini, P.A. Knolle, Living in the liver: hepatic infections, Nat. Rev. Immunol. 12 (3) (2012) 201–213.
[48] E. Raz, Organ-specific regulation of innate immunity, Nat. Immunol. 8 (1) (2007) 3–4.
[49] J. Cui, S. Liu, B. Zhang, H. Wang, H. Sun, S. Song, X. Qiu, Y. Liu, X. Wang, Z. Jiang, Z. Liu, Transciptome analysis of the gill and swimbladder of Takifugu rubripes by RNA-Seq, PLoS One 9 (1) (2014) e85505.
[50] P.R. Rauta, B. Nayak, S. Das, Immune system and immune responses in fish and their role in comparative immunity study: a model for higher organisms, Immunol. Lett. 148 (1) (2012) 23–33.
[51] Y. Duan, J. Zhang, H. Dong, Y. Wang, Q. Liu, H. Li, Oxidative Stress Response of the

Black Tiger Shrimp Penaeus monodon to Vibrio Parahaemolyticus Challenge, (2015).
[52] K. Junkunlo, K. Soderhall, I. Soderhall, C. Noonin, Reactive oxygen species affect transglutaminase activity and regulate hematopoiesis in a Crustacean, J. Biol. Chem. 291 (34) (2016) 17593–17601.
[53] B. Paital, G.B.N. Chainy, Effects of salinity on O-2 consumption, ROS generation and oxidative stress status of gill mitochondria of the mud crab Scylla serrata, Comp. Biochem. Physiol. C 155 (2) (2012) 228–237.
[54] S. Thitamadee, J. Srisala, S. Taengchaiyaphum, K. Sritunyalucksana, Double-dose beta-glucan treatment in WSSV-challenged shrimp reduces viral replication but causes mortality possibly due to excessive ROS production, Fish Shellfish Immunol. 40 (2) (2014) 478–484.
[55] L. Wang, T. Xu, W.W. Lei, D.M. Liu, Y.J. Li, R.J. Xuan, J.J. Ma, Cadmium-induced oxidative stress and apoptotic changes in the testis of freshwater crab, sinopotamon henanense, PLoS One 6 (11) (2011).
[56] I. Banmeyer, C. Marchand, A. Clippe, B. Knoops, Human mitochondrial peroxiredoxin 5 protects from mitochondrial DNA damages induced by hydrogen peroxide, FEBS Lett. 579 (11) (2005) 2327–2333.
[57] K.W. Kim, I.H. Kim, K.Y. Lee, S.G. Rhee, E.R. Stadtman, The isolation and purification of a specific protector protein which inhibits enzyme inactivation by a thiol/Fe(iii)/O-2 mixed-function oxidation system, J. Biol. Chem. 263 (10) (1988) 4704–4711.
[58] Y.Z. Luo, E.S. Henle, S. Linn, Oxidative damage to DNA constituents by iron-mediated Fenton reactions - the deoxycytidine family, J. Biol. Chem. 271 (35) (1996) 21167–21176.
[59] C.A. Neumann, D.S. Krause, C.V. Carman, S. Das, D.P. Dubey, J.L. Abraham, R.T. Bronson, Y. Fujiwara, S.H. Orkin, R.A. Van Etten, Essential role for the peroxiredoxin Prdx1 in erythrocyte antioxidant defence and tumour suppression, Nature 424 (6948) (2003) 561–565.
[60] K. Saranya Revathy, N. Umasuthan, I. Whang, H.B. Jung, B.S. Lim, B.H. Nam, J. Lee, A potential antioxidant enzyme belonging to the atypical 2-Cys peroxiredoxin subfamily characterized from rock bream, Oplegnathus fasciatus, Comp. Biochem. Physiol. B Biochem. Mol. Biol. 187 (2015) 1–13.
[61] L. Wu, Y. Zhou, M.N. Abbas, S. Kausar, Q. Chen, C.-X. Jiang, L.-S. Dai, Molecular structure and functional characterization of the peroxiredoxin 5 in Procambarus clarkii following LPS and Poly I:C challenge, Fish Shellfish Immunol. 71 (2017) 28–34.
[62] L.-S. Dai, X.-M. Yu, M.N. Abbas, C.-S. Li, S.-H. Chu, S. Kausar, T.-T. Wang, Essential role of the peroxiredoxin 4 in Procambarus clarkii antioxidant defense and immune responses, Fish Shellfish Immunol. 75 (2018) 216–222.
[63] T.T. Priyathilaka, Y. Kim, H.M.V. Udayantha, S. Lee, H.M.L.P.B. Herath, H.H.C. Lakmal, D.A.S. Elvitigala, N. Umasuthan, G.I. Godahewa, S.I. Kang, H.B. Jeong, S.K. Kim, D.J. Kim, B.S. Lim, Identification and molecular characterization of peroxiredoxin 6 from Japanese eel (Anguilla japonica) revealing its potent antioxidant properties and putative immune relevancy, Fish Shellfish Immunol. 51 (2016) 291–302.
[64] R.N.N. Abskharon, S.H.A. Hassan, M.H. Kabir, S.A. Qadir, S.M.F.G. El-Rab, M.H. Wang, The role of antioxidants enzymes of E. coli ASU3, a tolerant strain to heavy metals toxicity, in combating oxidative stress of copper, World J. Microbiol. Biotechnol. 26 (2) (2010) 241–247.
[65] R. Bu, P. Wang, C. Zhao, W. Bao, L. Qiu, Gene characteristics, immune and stress responses of PmPrx1 in black tiger shrimp (Penaeus monodon): insights from exposure to pathogenic bacteria and toxic environmental stressors, Dev. Comp. Immunol. 77 (2017) 1–16.